

Optimizing Thomson's jumping ring

Paul J. H. Tjossem and Elizabeth C. Brost

Department of Physics, Grinnell College, Grinnell, Iowa 50112

(Received 21 May 2010; accepted 14 September 2010)

The height to which rings will jump in a Thomson jumping ring apparatus is the central question posed by this popular lecture demonstration. We develop a simple time-averaged inductive-phase-lag model for the dependence of the jump height on the ring material, its mass, and temperature and apply it to measurements of the jump height for a set of rings made by slicing copper and aluminum alloy pipe into varying lengths. The data confirm a peak jump height that grows, narrows, and shifts to smaller optimal mass when the rings are cooled to 77 K. The model explains the ratio of the cooled/warm jump heights for a given ring, the reduction in optimal mass as the ring is cooled, and the shape of the mass resonance. The ring that jumps the highest is found to have a characteristic resistance equal to the inductive reactance of the set of rings. © 2011 American Association of Physics Teachers.

[DOI: 10.1119/1.3531946]

I. INTRODUCTION

Thomson's ac jumping ring¹ is a mainstay of physics lecture demonstrations² invoking Faraday's law and is often enhanced by chilling the rings with liquid nitrogen.³ A conducting ring placed over the extended core of a vertical solenoid will jump in the air when the primary circuit is connected to an ac power line (see Fig. 1). The nature of the jump defies a simple Lenz law interpretation,⁴ and the interplay between the ring's inductance and resistance can be dramatic and puzzling: two or three rings together will often jump higher than one; a copper ring that barely moves by itself will jump vigorously when weighted down by an aluminum ring placed on top of it, moving together despite the greater density of the copper. A small ring chilled in liquid nitrogen jumps much higher than its reduced resistance would suggest, but some larger rings will jump no higher upon chilling. To these effects Baylie *et al.*⁵ added this latest puzzle: the jump height as a function of ring mass shows a resonance that varies with mass and temperature.

In this paper we confirm the mass resonance for copper and aluminum alloy rings of tubular geometry. We find the inductance of the rings to be independent of their axial length and exploit this simplification to develop a time-averaged inductive-phase-lag model that explains all of the observations for any material at any temperature. We examine several limiting cases that serve to enhance the demonstration.

II. THEORY

The Lorentz force on the floating ring arises from the interaction between the circumferential current induced in the ring by the large axial alternating magnetic field of the solenoid and the radial component of the solenoid's fringing magnetic field. The derivation of the electromagnetic force on the floating ring is given in Refs. 6 and 7, where it is shown that the time-averaged upward electromagnetic force on the ring can be written as

$$\langle F \rangle = I^2 \{S(z)\} \sin^2 \delta = I^2 \{S(z)\} \frac{1}{(R/\omega L)^2 + 1}, \quad (1)$$

where I is the ac in the solenoid, $S(z)$ represents the spatial variation of the force with height z along the extended core,

independent of the ring's impedance, and the $\sin^2 \delta$ term is due to the inductive-phase-lag angle δ between the induced emf in the ring and its current. Equation (1) requires that $\delta \neq 0$ for there to be a nonzero time-averaged upward force. The phase lag depends on the ratio of the ring's inductive reactance to its resistance according to

$$\tan \delta = \frac{\omega L}{R}, \quad (2)$$

where ω is the natural frequency of the ac power source, R is the ring resistance, and L is the dressed (that is, core-enhanced) inductance of the ring while sitting on the iron core of the apparatus. Equation (1) assumes that the current in the solenoid has a fixed rms value. In practice, the jumping ring is usually powered with fixed rms voltage, but because the Thomson coil is a lossy step-down transformer that operates in the limit of weak coupling, the primary current does not vary appreciably with ring impedance.⁷

Rings of different axial lengths sliced from a metal pipe with constant wall thickness have a circumferential resistance that varies inversely with the length and might be expected to have an inductance that increases with length in a more complicated way.^{8,9} However, the design of the typical Thomson jumping ring apparatus is such that the dressed inductance (self and mutual) of a ring on the magnetic core is largely fixed for rings of nearly any length, as was found in Ref. 7 and confirmed recently.¹⁰ The inductance is fixed because most of the magnetic flux due to the ring current is effectively channeled by the core, so that longer rings do not capture any more of their own flux. In terms of magnetic energy, the volume of the region containing most of the magnetic field is fixed by the core and not by the ring. Thus, changing the length of the ring and thereby its conduction cross section mainly affects its resistance, greatly simplifying Eq. (1) so that the inductance remains fixed at L for any length ring while on the iron core of the apparatus.

The ring stays on the core for many quarter cycles of the alternating current in the solenoid, and thus the force in Eq. (1) can be considered to be steady over the time scale of a typical jump.^{7,10} The force delivers an impulse to the ring after which the ring undergoes free fall. The drop in the force with height is accounted for by the shape function $S(z)$, which reaches zero just after the end of the core (where

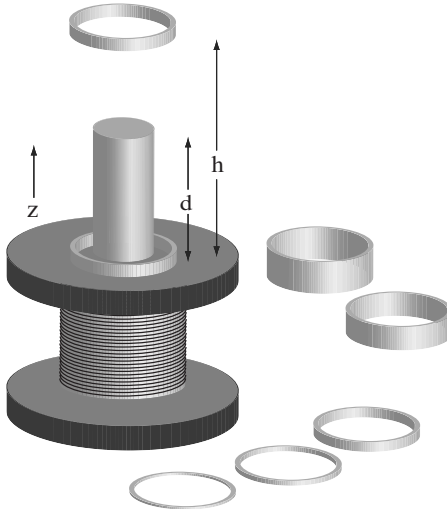


Fig. 1. The jumping ring apparatus consists of a solenoid, an iron core, and a set of rings of various axial lengths sliced from copper and aluminum alloy pipe of fixed wall thickness. The core was extended by $d=14$ cm for these measurements and the jump height h measured from the starting position of the ring.

$z=d$), mostly because the emf induced in the ring decreases with height and partly because the magnetic field has less of a radial component with increasing height.^{7,10,11} Thus, the work done on the jumping ring is due to the square of the solenoid current times the integral of $S(z)$ over a fixed interaction length (approximately the core extension d), which is the same for all rings, times a phase factor that varies with ring resistance. We ignore the rapid decline in the inductance of the ring just as it leaves the core because the majority of the work is done before any appreciable change in inductance occurs.⁷

With the simplification that the inductance L is independent of ring length, we define the characteristic ring resistance as

$$R_0 \equiv \omega L = X_L, \quad (3)$$

which is the inductive reactance X_L of the ring while on top of the core. This characteristic resistance has special significance for the jumping ring apparatus. We will show that a ring with this resistance, whose phase lag $\delta=45^\circ$, will jump higher than any other ring in a set of rings with fixed resistivity but differing mass. Note that X_L is still a function of the core dimensions, the ring diameter, and its wall thickness, and therefore we keep these parameters and the frequency ω fixed in the analysis that follows.

The mechanical work done by the electromagnetic force on a ring of resistance R over the length of the extended core d raises its gravitational potential energy to a maximum of mgh ,

$$W(R) = \int_0^d \langle F \rangle dz = I^2 \left\{ \int_0^d S(z) dz \right\} \sin^2 \delta \quad (4a)$$

$$= I^2 S \frac{1}{(R/R_0)^2 + 1} = mgh, \quad (4b)$$

where S is a constant defined implicitly in Eq. (4), m is the ring mass, and h is the jump height measured from the starting position of the ring.

We define the standard ring to be the ring of mass m_0 and room-temperature resistivity ρ_0 that has the characteristic resistance R_0 of Eq. (3). This standard ring will have work

$$W(R_0) = I^2 S \frac{1}{(R_0/R_0)^2 + 1} = I^2 S \frac{1}{2} = m_0 g h_0 \quad (5)$$

done on it, causing it to jump to height h_0 . The resistance of any other ring in the set is directly proportional to its resistivity ρ and inversely proportional to its axial length or equivalently its mass,

$$R = R_0 \frac{m_0 \rho}{m \rho_0}. \quad (6)$$

We divide Eq. (4) by Eq. (5) and use Eq. (6) to obtain the normalized jump height for any ring in the set,

$$\frac{h}{h_0} = \left(\frac{m_0}{m} \right) \frac{2}{(R/R_0)^2 + 1} = \left(\frac{m_0}{m} \right) \frac{2}{((m_0/m)(\rho/\rho_0))^2 + 1}, \quad (7)$$

with the corresponding phase angle given by

$$\tan \delta = \frac{m/m_0}{\rho/\rho_0} = \frac{R_0}{R}. \quad (8)$$

The mechanical work $W(R)$ done on the ring depends only on R , whereas the height to which it jumps depends on both $W(R)$ and m . There are two independent ways to vary the ring's resistance: either by changing its resistivity or by changing its cross sectional area, that is, its mass.

If we fix the mass at $m=m_0$ and optimize Eq. (7) by changing the resistivity ρ (for example, by cooling), the normalized jump height monotonically reaches a maximum value of 2 as $\rho \rightarrow 0$. (Even for zero resistance, the ring current does not increase without limit—it is constrained by the inductance of the ring.) From Eq. (8) the phase angle then goes to 90° , which is the angle that maximizes the force on the floating ring.⁷ If, instead, we optimize Eq. (7) with respect to the mass m at fixed resistivity $\rho=\rho_0$ (that is, by slicing a ring of different axial length), the normalized jump height peaks at 1 when $m=m_0$, which is the standard ring with characteristic resistance R_0 . Equation (8) then becomes

$$\tan \delta = \frac{m \rho_0}{m_0 \rho} = 1, \quad (9)$$

corresponding to the optimal phase lag δ of 45° . This optimal phase shift for the jump was derived recently¹² and is the same angle that maximizes the force per unit weight of a collection of small floating rings of identical mass.⁷ Equation (7) should hold in the impulse approximation for short rings (axial length < diameter) of various lengths sliced from thin-walled homogeneous pipe of fixed diameter and wall thickness. Schneider and Ertel¹³ found a similar expression [their Eq. (14)] but obscured the simplicity of the apparatus by assuming that the ring inductance followed Nagaoka's (air-core) expressions.⁸

The optimal mass and the width of the mass resonance result from two competing tendencies: at $\delta=0^\circ$ there is no time-averaged Lorentz force on the ring (the force would alternate up and down every 1/4 cycle of the alternating current, and all the power would be dissipated as Joule heating of the ring).^{4,7} In contrast, the maximum time-averaged Lorentz force occurs as $R \rightarrow 0$, $\delta \rightarrow 90^\circ$. The added mass needed to reduce the resistance in order to approach this limit even-

tually lowers the jump height.⁷ If we express the normalized jump height in Eq. (7) using Eqs. (1) and (8) and exclude $\rho=0$, we obtain

$$\frac{h}{h_0} = 2 \frac{m_0}{m} \sin^2 \delta = 2 \frac{m_0}{m} \sin \delta \frac{\sin \delta}{\cos \delta} \cos \delta \quad (10a)$$

$$= 2 \frac{m_0}{m} \sin \delta \left(\frac{m \rho_0}{m_0 \rho} \right) \cos \delta \quad (10b)$$

$$= 2 \frac{\rho_0}{\rho} \sin \delta \cos \delta = \frac{\rho_0}{\rho} \sin 2\delta, \quad (10c)$$

which reaches a maximum of ρ_0/ρ at $\delta=45^\circ$. The derivation leading to Eq. (10c) needs to exclude $\rho=0$ to avoid division by zero. In that case, $\delta=90^\circ$ and hence $h/h_0=2m_0/m$ from Eq. (7), and there is no resonance except for the singularity at $m=0$.

In terms of angles, Eq. (10c) reaches its half-values when $\sin 2\delta=1/2$ or 15° and 75° . In terms of mass, at fixed $\rho=\rho_0$, Eq. (7) falls to half of its peak value where

$$\frac{m}{m_0} = (2 \pm \sqrt{3}) = \arctan(45^\circ \pm 30^\circ) \cong 0.27, 3.73. \quad (11)$$

Thus, we expect to see an asymmetric resonance centered at m_0 , with full width at half maximum $\Delta m=2\sqrt{3}m_0$, which tails toward the high mass side of the peak.

Three limiting cases illustrate the expected behavior of the jumping ring as its resistance changes:

Peak heights for warm and cold rings. If the standard ring ($m=m_0$) is chilled in liquid nitrogen, its resistivity falls from ρ_0 to ρ such that

$$\frac{\rho_0}{\rho} = \frac{\rho_{295 \text{ K}}}{\rho_{77 \text{ K}}} = \alpha, \quad (12)$$

and Eq. (7) shows that it will jump higher, to $2\alpha^2/(\alpha^2+1)$, but no more than twice the standard height even if $\alpha \rightarrow \infty$, allowing the demonstrator to reject any notion that the jump height is proportional to the resistivity ratio.⁵ Reducing the mass to m_0/α restores δ to 45° via Eq. (9),

$$\frac{m \rho_0}{m_0 \rho} = \frac{m}{m_0} \alpha = 1, \quad (13)$$

where its resistance is R_0 . This shorter ring of mass $m=m_0/\alpha$ gives

$$h = h_0 \left(\frac{m_0}{m} \right) \frac{2}{((m_0/m)(1/\alpha))^2 + 1} = h_0 \left(\frac{m_0}{m} \right) = \alpha h_0, \quad (14)$$

so that the new smaller ring will jump α times higher, which is the warm/cold resistivity ratio. This result follows directly from the work-energy theorem: the smaller chilled ring, having the same resistance R_0 as the standard ring, has the same mechanical work $W(R_0)=m_0gh_0$ done on it, but because it has $1/\alpha$ times the mass, it jumps α times higher. The product of optimal ring mass m_0 and peak jump height h_0 is thus a constant of the apparatus for a set of rings of any material and temperature fixed by $W(R_0)$.

Cold/warm jump ratio for a cold-optimized ring. For the cold-optimized ($m=m_0/\alpha$) ring, the ratio of jump heights for cold versus warm rings can become quite large,

$$\frac{h_{\text{cold}}}{h_{\text{warm}}} = \frac{h_0(m_0/m)\{2/[(1)^2 + 1]\}}{h_0(m_0/m)\{2/[(m_0/m)(\rho_0/\rho_0))^2 + 1]\}} = \frac{\alpha^2 + 1}{2}, \quad (15)$$

a ratio that exceeds α for any $\alpha > 1$. A cold-optimized aluminum alloy ring whose resistivity falls by a factor of 3 ($\alpha=3$, $m=m_0/3$) will jump five times higher when chilled. A cold-optimized copper ring, whose resistivity falls by a factor of 7 upon chilling in liquid nitrogen, will jump 25 times higher than at room temperature, providing a more impressive demonstration than the approximately two times improvement in the standard ($m=m_0$) ring.

Mass for which the cold/warm jump ratio equals α . If a ring is sized so that

$$m_1 = \frac{m_0}{\sqrt{\alpha}}, \quad (16)$$

it is neither optimized for the warm nor the cold, but it will jump to a height $h_1=2h_0\sqrt{\alpha}/(\alpha+1)$ given by Eq. (7) at room temperature. Upon being cooled to 77 K the jump height becomes $2h_0\alpha\sqrt{\alpha}/(\alpha+1)=\alpha h_1$ for the same ring. This ring is both $\sqrt{\alpha}$ smaller than the standard ring and $\sqrt{\alpha}$ larger than the cold-optimized ring. Only for this specially sized ring can the demonstrator say that the increased jump height is directly proportional to the increased conductivity of the material.

III. EXPERIMENTS

As discussed by numerous authors, most recently Bostock-Smith,¹² aluminum is traditionally preferred to copper in the jumping ring demonstration because its density is 3.3 times lower but its resistivity is 1.6 times higher, which permits double the peak jump height at room temperature.¹⁴ The resistivity of aluminum or its alloys (α is in the range of 2–15) at 77 K is highly dependent on composition, work hardening, aging, and annealing.^{15,16} Baylie *et al.* pointed out the importance of annealing a new aluminum ring so that it will jump as high as an old one.¹⁷ Depending on how hot the rings are while being machined or the subsequent inductive heating of the ring, the rings undergo periodic heating/cooling cycles. A tempered aluminum jumping ring probably partially anneals itself if held down long enough on the apparatus. (One of the typical demonstrations is to see how long a student can hold a powered ring down by hand—the answer is not long because the ring currents can be hundreds of amperes, leading to rapid Joule heating.¹⁸) Hence, a well-used older ring will likely have lower resistivity.

For these measurements the more predictable electrical properties of oxygen-free high-conductivity copper¹⁴ enabled us to confirm the cold/warm jump behavior while avoiding the need for heat treating. Copper rings were gently machined from seamless pipe stock (50.8 mm outer diameter, 3.18 mm wall thickness, and 0.35–28.5 mm length)¹⁹ and used without further annealing. For comparison, we used 6061-T6 pipe, a readily available heat-treatable aluminum alloy of the same dimensions, although 6063-T52, with fewer impurities, is likely to be a better choice. (Pure elemental aluminum, with $\alpha \approx 15$, would be better still but is too soft to be readily available in pipe form.)

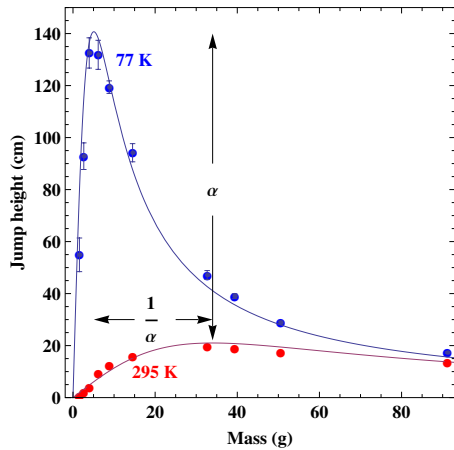


Fig. 2. The jump height for cold and room-temperature copper rings fitted to Eq. (7) at room temperature and Eq. (14) with the warm/cold resistivity ratio $\alpha=6.7$ at 77 K. The work-energy theorem locks the two curves together as shown, reducing the optimal mass by a factor of α while increasing the peak jump by α . For rings of mass $m < m_0/\sqrt{\alpha}$, the cold/warm jump height ratio exceeds α .

The 6061-T6 rings were machined, annealed at 415 °C for 2 h, then allowed to cool slowly to room temperature. Annealing the 6061 rings left their room-temperature resistance nearly unchanged but increased α from 3 to 4. The resistivity of the rings was measured with a four-wire sourcemeter/nanovoltmeter (Keithley 2400/2182) operated in current-reversal mode, whereby thermal contact potentials are averaged out. For our copper pipe the room-temperature resistivity ρ_0 was $1.8 \pm 0.2 \mu\Omega \text{ cm}$ and upon cooling, $\alpha=6.8 \pm 0.6$. The 6061-O (annealed) rings had $\rho_0=3.3 \pm 0.3 \mu\Omega \text{ cm}$ and $\alpha=4.0 \pm 0.4$.

The CENCO Thomson coil was operated at 75 VAC to keep the rings from bouncing off the ceiling, and the core was extended $d=14$ cm beyond the solenoid end cap. The rings were centered and kept cold prior to launching by setting them on a shallow chilled phenolic plastic tray (not shown in Fig. 1) that rested over the core and atop the solenoid end cap. Results for jump height as a function of mass for the copper rings, each of identical wall thickness, are shown at 295 and 77 K in Fig. 2. The room-temperature curve peaks at $m_0=32$ g and the chilled peak is 6.7 times higher and lies at 6.7 times lower mass, as predicted from the work-energy theorem via Eqs. (13) and (14). The smooth curves follow Eqs. (7) and (14) with a fitted value of $\alpha=6.7$, in agreement with our measured resistance ratio for copper and from published data (6.7:1).^{14,20} Annealed 6061 alloy rings behaved similarly with a lower $\alpha=4.0$. The aluminum rings had 1.8 times the optimal jump height as copper at room temperature. This result follows from Eq. (7). To achieve R_0 at room temperature, the alloy ring needed to be $\rho_{\text{Al}6061-\text{O}}/\rho_{\text{Cu}}=1.8$ times longer than the standard copper ring, but because its density is 3.3 times lower, it had $1.8/3.3=0.55$, the mass of the standard copper ring, and hence jumped $1/0.55=1.8$ times as high.^{14,15}

Rings that jumped less than 14 cm did not clear the extended core and thus did not receive the full measure of work done on them according to Eq. (4). If we use the measured room-temperature resistivity of our copper rings, we find that $R_0=\omega L=9.8 \times 10^{-5} \Omega$ for our apparatus and set of rings. This relation gives $L=2.6 \times 10^{-7} \text{ H}$, a few times larger than

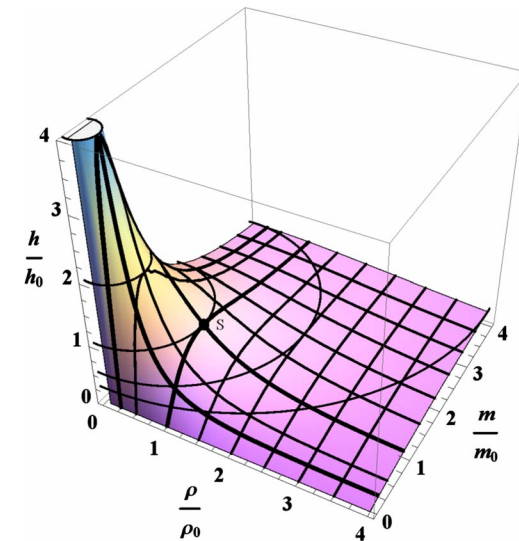


Fig. 3. Normalized jump height as a function of normalized mass and resistivity, showing the semicircular level surfaces and the increasingly sharp mass resonance as resistivity is reduced. The jump height reaches a maximum for a given resistivity at $m/m_0=\rho/\rho_0$, where $\delta=45^\circ$. The standard ring lies at $S=(1,1,1)$.

the calculated free-space value for the standard ring⁹ and consistent with a relative permeability of $\mu_r \approx 3$, as found for other Thomson coils.^{7,13,21,22} Under typical operating conditions, the peak jump height of the cold-optimized copper ring at 143 VAC was $4.4 \pm 0.6 \text{ m}$, in agreement with the scaling expected from the $(143 \text{ VAC}/75 \text{ VAC})^2$ ratio, showing that air resistance is negligible.

IV. DISCUSSION

The simple inductive-phase-lag model, developed under the assumptions of constant solenoid current, fixed ring inductance, and fixed electromagnetic interaction length, fits our data for both warm and chilled rings except at the extremes of high mass (length) where the dressed inductance of the ring is expected to drop²³ and the interaction length is reduced as the middle of the ring starts higher above the center of the apparatus. A key finding is that the ring inductance is independent of the axial length for rings of fixed wall thickness and diameter. The ring that jumps the highest for a given resistivity is the one whose resistance is equal to the characteristic resistance $R_0=\omega L$, as given by Eq. (3), and whose inductive-phase-lag angle is 45° . Rings shorter than $1/\sqrt{\alpha}$ times the optimal room-temperature length make particularly spectacular jumps when chilled in liquid nitrogen, far exceeding their warm/cold resistivity ratio.

A. A further puzzle: The phase angle

The two different phase angles ($45^\circ, 90^\circ$) that optimize Eq. (7), depending on whether we vary mass (via axial length) or resistivity (via temperature), are initially disconcerting. In a two-dimensional space (varying m or varying resistivity ρ), the mass parameter implicitly contains the resistance, whereas the other axis is independent of the mass. We plot the normalized jump height in Eq. (7) as a function of the normalized mass m/m_0 and the normalized resistivity ρ/ρ_0 in Fig. 3. The standard ring (S) lies at $(1,1,1)$. Equation

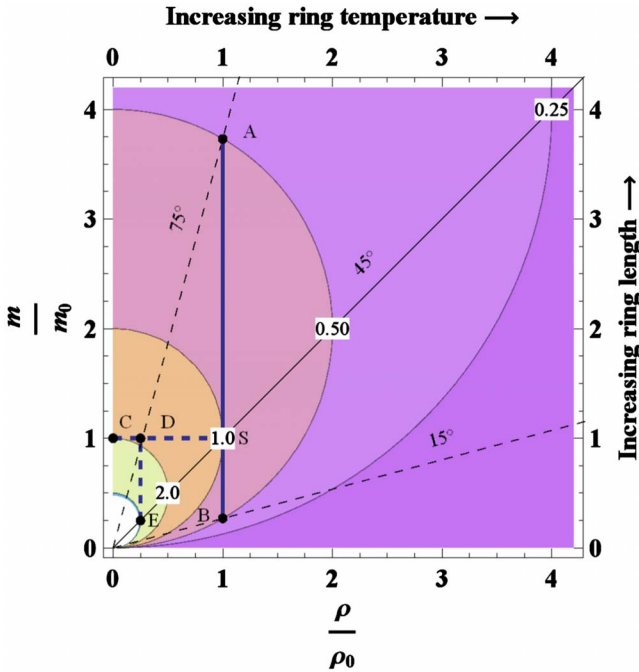


Fig. 4. Contours of normalized jump height as a function of normalized mass and resistivity form semicircles (see the Appendix). Angles measured from the resistivity axis are the phase lag δ . The standard ring lies at S , where the $\delta=45^\circ$ line crosses the 1.0 contour. Moving up or down the m/m_0 axis cuts the jump height in half at points A or B . Moving toward lower resistivity at most doubles the jump height at C . A factor of 4 drop in resistivity results in a slightly higher jump at higher phase lag (D) and reducing the mass by a factor of 4 restores the optimal phase angle to $\delta=45^\circ$, resulting in four times the jump height at E .

(8) shows that angles on this plot are the phase lag δ ; that is, we replace the usual complex $i\omega L$ axis on a phasor diagram by m/m_0 and the usual real resistance axis by ρ/ρ_0 . Cooling a ring changes its resistivity without affecting its mass and results in a displacement parallel to the ρ/ρ_0 axis. A set of rings made of fixed resistivity but different masses will fall on a line parallel to the m/m_0 axis, similar to the measurements in Fig. 2. In this mapping, all rings with the characteristic resistance R_0 lie on the 45° line, satisfying Eq. (9). The normalized jump height in Fig. 3 shows the mass resonance for a set of rings at constant resistivity, the peak at 45° , and the narrowing of the peak as the resistivity drops.

Figure 4 is a contour plot of the same normalized jump height and shows more clearly the semicircular contours. The figure of merit for a given ring material is the reciprocal of the product of its mass and resistivity,¹² which in dimensionless form becomes

$$\frac{m_0 \rho_0}{m \rho} = p^2 \quad (17)$$

for some constant p . Contours of equal height form semicircles (see the Appendix) of radius $1/p$ centered at $(0, 1/p)$, each having normalized jump height p . The standard ring (S) intersects the $h/h_0=1.0$ contour at $(1, 1)$. Increasing its mass moves the ring toward A , where using Eq. (11), it intersects the $1/2$ contour at $\delta=75^\circ$ for a normalized mass $m/m_0=(2+\sqrt{3})$. Reducing the ring mass (along line SB) brings it to $m/m_0=(2-\sqrt{3})$ and on the $1/2$ contour at $\delta=15^\circ$. Returning to S , we move parallel to the ρ/ρ_0 axis by

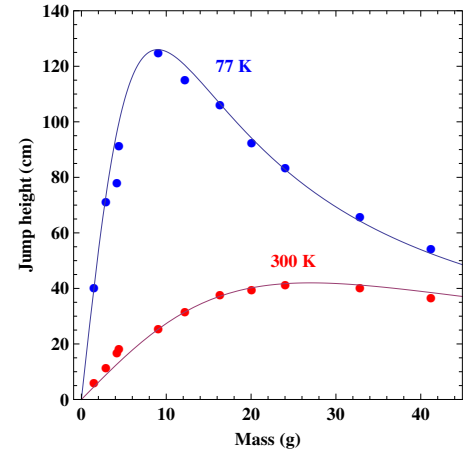


Fig. 5. Jump height data for cold and room-temperature aluminum rings, taken from Ref. 5 and fitted to Eq. (7) at room temperature and with Eq. (14) and $\alpha=3.0$ at 77 K.

changing the resistivity along line SC , where the height function increases monotonically toward 2.0 but does not reach it unless $\rho=0$ at $\delta=90^\circ$. For $\rho \neq 0$, however, moving down the mass axis reduces the phase toward the optimal $\delta=45^\circ$. In doing so, we pass through several higher jump contours. For example, if we cut the resistivity by a factor of 4 (point D), we can cut the mass by a factor of 4, which intersects the 45° line at the 4.0 contour E , indicating that the ring will jump four times as high as the standard $m=m_0$ ring. The half-heights of the resonance still occur at 15° and 75° but extend over a narrower mass range than before because the product of the maximum normalized jump height and the normalized width is a constant, that is, $p\Delta m/m_0=2\sqrt{3}$. There is no such resonance with changing resistivity alone. Ultimately, there is only one optimal phase-lag angle for the jumping ring, $\delta=45^\circ$.

B. Comparison to other work

A recent paper⁵ provides an excellent independent set of jump height data at room temperature and 77 K. Figure 4 in Ref. 5 shows the jump height of a set of aluminum (unspecified alloy) rings of fixed diameter and wall thickness. The data in Ref. 5 are shown in Fig. 5. It is commented that “the response is much flatter at room temperature and the maximum (as well as can be detected) occurs in rings of higher mass. The reasons for this are not well understood.”⁵ We now provide an explanation. A fit of the normalized jump height in Eq. (7) to these data at room temperature yields $h_0=42$ cm at $m_0=27$ g. Cooling the rings of Ref. 5 in liquid nitrogen reduces their resistivity by α , and therefore the rings need to be shortened accordingly, shifting the peak jump to mass $m_{\text{cold}}=9$ g. Hence,

$$\alpha = \frac{m_{\text{warm}}}{m_{\text{cold}}} = \frac{27 \text{ g}}{9 \text{ g}} = 3, \quad (18)$$

so that the peak jump becomes 3×42 cm = 126 cm by Eq. (14). The three-parameter fit (h_0, m_0, α) using Eqs. (7) and (14) matches their results at both temperatures, confirming the general applicability of the model.

C. Optimizing your own apparatus

It is necessary to find the peak jump height at room temperature to determine the mass m_0 of the standard ring. Rather than a series of rings, we could slice two rings of different lengths and measure their jump heights alone and then stacked together. Two rings behave as one because their parallel currents (and similar phase shifts) keep them together even if they have dissimilar density. Two different temperatures and six jump heights will provide more than enough data to determine the parameters h_0 , m_0 , and α . If the resistivity ratio α is known from a separate measurement, a single ring with jump heights h_1 and h_2 at room temperature and at 77 K can be used via Eqs. (7) and (14) to find m_0 and map out the entire mass/resistivity parameter space.

ACKNOWLEDGMENTS

The authors would like to thank W. B. Case for many helpful discussions and S. Peterson for assistance with the figures.

APPENDIX: DERIVATION OF CONTOUR HEIGHT

The shape and height of the contours of normalized jump height [Eq. (7)] shown in Fig. 4 can be found by setting $x \equiv \rho/\rho_0$ and $y \equiv m/m_0$, yielding

$$\frac{h}{h_0} = \frac{2/y}{(x/y)^2 + 1}. \quad (\text{A1})$$

If we combine Eq. (A1) with the figure of merit from Eq. (17) for a given ring material, $(m/m_0)(\rho/\rho_0) = yx = 1/p^2$, and eliminate x , we obtain

$$\frac{h}{h_0} = \frac{2/y}{(1/p^2 y^2)^2 + 1}. \quad (\text{A2})$$

At the optimal phase angle of 45°, $py=1$ and thus $h/h_0=p$. Then, the normalized jump height for any (x,y) coordinate can be written as

$$p = \frac{2/y}{(x/y)^2 + 1} \quad (\text{A3})$$

and hence

$$x^2 + y^2 = \frac{2y}{p}. \quad (\text{A4})$$

Letting $y \rightarrow y' + 1/p$ gives

$$x^2 + y'^2 = \frac{1}{p^2}, \quad (\text{A5})$$

showing that the plot of m/m_0 versus ρ/ρ_0 yields (semi)circular contours of height p , radius $1/p$, and offset up the mass axis by $1/p$.

- ¹E. Thomson, "Novel phenomena of alternating currents," *The Electrician* (London, June 10, 1887), n.p.
- ²Physics Instructional Resource Association (PIRA) demonstration bibliography, 5K20.30 (physicslearning.colorado.edu/PIRA/pira.asp).
- ³P. J. Ford and R. A. L. Sullivan, "The jumping ring revisited," *Phys. Educ.* **26**, 380–382 (1991).
- ⁴E. J. Churchill and J. D. Noble, "A demonstration of Lenz's law?," *Am. J. Phys.* **39**, 285–287 (1971).
- ⁵M. Baylie, P. J. Ford, G. P. Mathlin, and C. Palmer, "The jumping ring experiment," *Phys. Educ.* **44**, 27–32 (2009).
- ⁶W. M. Saslow, "Electromechanical implications of Faraday's law: A problem collection," *Am. J. Phys.* **55**, 986–993 (1987).
- ⁷P. J. H. Tjossem and V. Cornejo, "Measurements and mechanisms of Thomson's jumping ring," *Am. J. Phys.* **68**, 238–244 (2000).
- ⁸H. Nagaoka, "The inductance coefficients of solenoids," *J. Coll. Sci., Imp. Univ. Tokyo* **27** (6), 1–33 (1909).
- ⁹Frederick W. Grover, *Inductance Calculations: Working Formulas and Tables* (Dover, New York, 1946), pp. 95–113.
- ¹⁰R. N. Jeffery and F. Amiri, "The phase shift in the jumping ring," *Phys. Teach.* **46**, 350–357 (2008).
- ¹¹J. Hall, "Forces on the jumping ring," *Phys. Teach.* **35**, 80–83 (1997).
- ¹²J. M. Bostock-Smith, "The jumping ring and Lenz's law: An analysis," *Phys. Educ.* **43**, 265–269 (2008).
- ¹³C. S. Schneider and J. P. Ertel, "A classroom jumping ring," *Am. J. Phys.* **66**, 686–692 (1998).
- ¹⁴David R. Lide, *Handbook of Chemistry and Physics*, 66th ed. (CRC Press, Boca Raton, FL, 1985), p. E-88.
- ¹⁵Joseph R. Davis, *Aluminum and Aluminum Alloys* (American Society for Metals, Metals Park, OH, 1993), pp. 319, 641, and 686.
- ¹⁶Heat treatment and workability, AL01 (www.mcmaster.com).
- ¹⁷A T6 temper is applied (Refs. 15 and 16) to 6061 alloy by heating it to 160 °C and holding it for 18 h, followed by air cooling. Conversely, we can destroy this temper by raising the aluminum to 413 °C for 2 h, then slowly cooling to below 260 °C.
- ¹⁸K. E. Jesse, "Measuring current in a jumping ring," *Phys. Teach.* **35**, 198–199 (1997).
- ¹⁹(www.onlinemetals.com).
- ²⁰*Electrical Resistivity Handbook*, edited by G. T. Dyos and T. Farrell (Peregrinus, London, 1992), p. 207.
- ²¹P. Tanner, J. Loebach, J. Cook, and H. D. Hallen, "A pulsed jumping ring apparatus for demonstration of Lenz's law," *Am. J. Phys.* **69**, 911–916 (2001).
- ²²S. Y. Mak and K. Young, "Floating metal ring in an alternating magnetic field," *Am. J. Phys.* **54**, 808–811 (1986).
- ²³Long cold rings jump a little higher than predicted by the model. As noted (Ref. 7) the relative permeability drops as the ring leaves the core, lowering L and characteristic resistance R_0 , thus favoring longer and colder rings.